Traceable Characterization of Broadband Pulse Waveforms Suitable for Cryogenic Josephson Voltage Applications

Alirio S. Boaventura[1], Dylan F. Williams[1], Gustavo Avolio[2] and Paul D. Hale[1]

[1]National Institute of Standards and Technology, USA
[2]KU Leuven, Belgium

***Abstract* — We characterize broadband pulse waveforms using a large signal network analyzer (LSNA) and a sampling oscilloscope, both calibrated to the same reference plane and traceable to the NIST Electro-Optic Sampling System (EOS). The waveforms under test are passed through the LSNA test set and fed into the oscilloscope, allowing measurements to be carried out without disconnecting the measurement instruments, which reduces the measurement uncertainty. We calibrate the LSNA for operation with an external broadband pulse source and we correct the oscilloscope measurements for time-base distortion, impedance mismatch and the complex frequency response of the oscilloscope's sampler. We characterize several pulse waveforms and show good agreement between the LSNA and the oscilloscope measurements. The techniques presented will be applied in the characterization of cryogenic waveforms generated by NIST Josephson arbitrary waveform synthesizer (JAWS) systems.**

***Index Terms* — Pulse waveform characterization, LSNA, sampling oscilloscope, voltage standards, JAWS system.**

I. Introduction

The NIST Quantum Voltage Project has traditionally developed and disseminated superconducting voltage standards for DC and audio metrology applications. These standards use 4 Kelvin cryogenically-cooled Josephson junctions (JJs) which generate quantum-accurate voltage pulses. The AC standard is called the Josephson Arbitrary Waveform Synthesizer (JAWS) [1]-[2]. To target wireless communications metrology, NIST is currently researching superconducting voltage standards at microwave frequencies.

To accurately characterize and de-embed cryogenic microwave waveforms generated by a superconducting source, a calibrated measurement instrument such as a large signal network analyzer (LSNA) will be required. As a first step toward traceable characterization of cryogenic microwave waveforms, in this work we compare broadband waveform measurements performed with an LSNA and a sampling oscilloscope at room temperature. This comparison increases the confidence in our measurement setup and sets the basis for future cryogenic waveform characterization.

Similar comparison studies exist [3]-[6]. Compared to those papers: 1) we fully calibrate both measurement instruments to the same reference plane; 2) we perform the measurements without disconnecting the measurement instruments, which reduces the measurement uncertainty; 3) we use the NIST Microwave Uncertainty Framework (MUF) to capture correlations in components of measurement uncertainty and transform them between frequency and time domains.

II. The Measurement Setup

Fig. 1 shows the measurement setup used to characterize broadband pulse waveforms with an LSNA and a sampling oscilloscope both calibrated to the same reference plane and traceable to NIST electro-optic sampling system. During the measurement phase, the internal CW test signal of the LSNA was replaced with an external signal, generated either by an arbitrary waveform generator (AWG) or by a comb generator. This signal was passed through the LSNA test set and fed into the oscilloscope via the LSNA test port 3.

Synchronization is key in this setup, as all equipment including the LSNA (Keysight PNA-X N5245A)[1], AWG (Keysight M8195A), sampling oscilloscope (Keysight sampling head 86118A), and external phase references

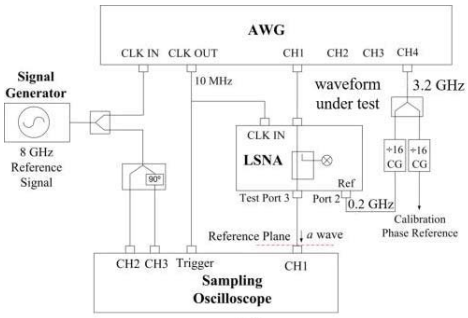

(a)

(b)

Fig. 1 a) Diagram of the measurement setup. b) Photograph of the measurement setup.

[1] Certain commercial equipment, instruments, or materials are identified in this paper to specify the experimental procedure adequately. Such identification is not intended to imply recommendation or endorsement by the National Institute of Standards and Technology, nor is it intended to imply that materials or equipment identified are necessarily the best available for the purpose.

U.S. Government work not protected by U.S. copyright

(Keysight comb generators U9391F) must be locked to the same reference signal. An 8 GHz sine-wave signal generated by an external signal generator (Agilent 8365L) was used as the master reference signal to which all the other were locked.

In addition to generating the waveform of interest on channel 1, the AWG was used to synchronously trigger the sampling oscilloscope and to clock the LSNA with its 10 MHz output clock signal, and to drive the comb generators (CG) with a 3.2 GHz signal generated on channel 4. An in-phase and quadrature (IQ) version of the 8 GHz reference signal was measured by the oscilloscope simultaneously with the waveform of interest and was used in post-processing by the NIST Time-Base Correction (TBC) algorithm to correct for jitter and other time-base distortions in the oscilloscope time-base [7]. Note that increasing the frequency of the IQ signal improves discrimination between jitter and voltage amplitude noise in the TBC algorithm.

III. Calibration And Measurement Correction

The full characterization of cryogenic microwave waveforms will require calibrated broadband measurements of the incident and reflected waves at the reference plane of the superconducting source using, for instance, an LSNA. As a first step, we compared room temperature measurements performed with an LSNA operated with an external broadband pulse source and a sampling oscilloscope. To compare the incident and reflected waves measured by the two instruments, they were calibrated to the same reference plane (Figs. 2-3). Note that the oscilloscope only measures the incident wave directly. The reflected wave can be calculated from the oscilloscope measurement of the incident wave and the oscilloscope reflection coefficient measured at the reference plane.

A. LSNA calibration

Fig. 2 illustrates the two-step procedure followed for broadband calibration and measurements with the LSNA:

1. The LSNA was first operated in its default configuration where the internal CW sources were used for scattering-parameter, absolute amplitude, and absolute phase calibrations. This is sketched in Fig. 2a. For the scattering-parameter and amplitude calibrations, the CW sources were swept across the desired harmonic frequency grids (from 0.2 GHz to 50 GHz with a step of 0.2 GHz for the 0.2 GHz signals and from 1 GHz to 50 GHz with a step of 1 GHz for the 1 GHz signals). For the absolute phase calibration, the comb generators were driven with a 3.2 GHz signal (generated on the AWG channel 4), and their divide ratios were set to 16, defining a frequency resolution of 0.2 GHz;
2. During the measurement of the waveform of interest, the switching circuitry of port 3 was routed to the external pulse source connected to the LSNA back-panel (see Fig. 2b). Note that changing the source configuration does not affect the calibration performed in step 1, because the full wave calibration matrix is independent of the source [8].

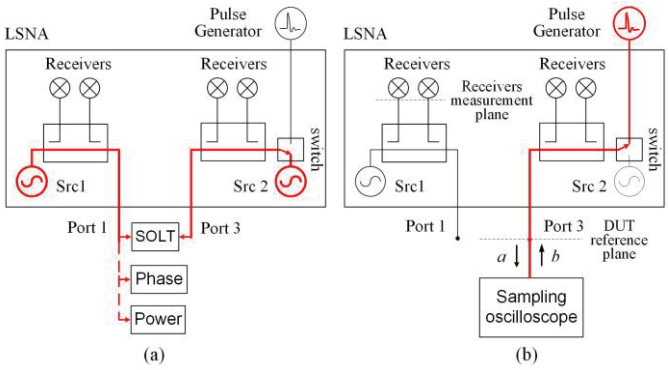

Fig. 2 a) Full wave calibration using the LSNA internal CW sources. b) Measurement with an external source.

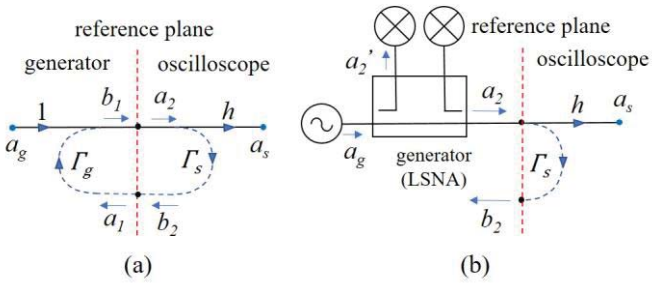

Fig. 3 a) Scope mismatch-corrected wave calibration. b) Calibration for the wave hitting the scope.

B. Sampling oscilloscope calibration

First, we used the NIST TBC algorithm to correct the time-base of the oscilloscope by using the auxiliary IQ signal measured on channels 2 and 3 [7]. Since the time vector after correction is not evenly spaced, the new waveform was interpolated to a uniform time grid prior to further processing.

Afterward, we used the MUF to correct the TBC data for the complex frequency response of the oscilloscope's sampler, which has been pre-characterized using a photo-diode calibrated by the NIST electro-optic sampling system (EOS) [9]-[10]. Note that the post-processor available in the MUF for oscilloscope data calibration usually corrects for the mismatch-corrected wave, a_g, delivered by a generator to the oscilloscope Eqn. (1), given the oscilloscope's complex impulse response, h, the measured raw data, a_s, and the reflection coefficients of the generator and oscilloscope, Γ_g and Γ_s (see Fig. 3a).

$$a_g = \frac{a_s}{h}(1 - \Gamma_g \Gamma_s) \quad (1)$$

To reuse this MUF post-processor to correct instead for the incident wave at the reference plane of the oscilloscope, a_2, we set Γ_g to zero so that $a_2 = a_g = a_s/h$ (Fig. 3b). A cable adaptor, not shown in Fig. 3 and not considered in Eqn. (1) for simplicity, was used to interconnect the oscilloscope head and the LSNA. To translate the oscilloscope data to the LSNA reference plane, the de-embedding of that cable was required.

Since the current impulse response characterization of the oscilloscope head has an arbitrary amplitude scaling, we further applied a correction scaling factor to the data given as the ratio of the magnitude of the LSNA fundamental component to the

magnitude of the oscilloscope's fundamental component, $\alpha = |a_{\mathrm{LSNA}}(\omega_0)|/|a_{\mathrm{Scope}}(\omega_0)|$. This scaling factor normalizes the amplitude of the oscilloscope data to the amplitude of LSNA's fundamental frequency component.

IV. Measurement Results

A. Measurement procedure

We characterized three waveforms: a 1 GHz square wave, a sinc-like waveform with a 1 GHz pulse repetition rate, and a broadband pulse signal with a 200 MHz pulse repetition rate. The first two signals were generated with a 25 GHz analog bandwidth AWG, and the third signal was generated by a broadband 50 GHz comb generator.

The comb waveform was used to exploit the 50 GHz measurement bandwidth of the LSNA. However, since this waveform has low average amplitude and the LSNA presents a large insertion loss from the back to front panel, the signal-to-noise ratio noticeably degraded, especially at higher frequencies, when the signal was passed through the LSNA test set. By using a calibrated Vector Network Analyzer (VNA), we measured the LSNA's back to front panel insertion loss at 50 GHz as being 22 dB for port 1 and 14 dB for port 3. Therefore, we chose to use port 3. To evaluate the impact of the LSNA test set on the comb waveform, we performed two different experiments. In the first experiment, we connected the comb generator directly to the oscilloscope. In the second experiment, we passed the comb signal through the LSNA test set and then we fed it into the oscilloscope via the LSNA test port 3. In both cases, we performed multiple oscilloscope measurements. The results are depicted in Fig. 4a and discussed in the next section.

The sinc-like test waveform intends to mimic the three-level sigma-delta modulated signal that is currently in use to bias the Josephson junction arrays of the NIST JAWS system [1]-[2]. For simplicity, we considered a periodic waveform with a single positive and negative pulse.

B. Discussion

The upper and lower curves in Fig. 4a show respectively the repeated oscilloscope measurements with the comb generator signal directly connected to the oscilloscope and going through the LSNA test set. These results show a noticeable degradation of the noise standard deviation when the signal is passed through the LSNA test set. This is due to the large insertion loss of the LSNA back-to-front signal path. To improve the noise performance, we reduced the LSNA IF bandwidth to 3 Hz and we averaged 1000 oscilloscope measurements.

Fig. 4b depicts the repeated oscilloscope measurements of the comb signal in the time-domain. The waveforms were then corrected for systematic and random jitter errors, by use of the NIST time-base correction (TBC) algorithm [7], interpolated to a uniform time grid, and averaged (black line). Fig. 4c shows the standard deviation of the 1000 waveforms before and after applying TBC. The same procedure was applied for the other two AWG waveforms. As the later signals have higher signal-to-noise ratio, only 100 repeated measurements were used.

Figures 5 through 7 compare the incident waves of the three measured signals after amplitude scaling, phase normalization and phase detrending. Since the LSNA and oscilloscope measurements are performed at different arbitrary times, phase normalization and phase detrending are important for aligning the waveforms.

The spectrum difference (in amplitude and phase) increases with frequency due a degradation in the signal-to-noise ratio, but the difference is relatively small up to 30 GHz. The time-domain difference is also relatively small. Table I presents the peak time-domain difference and the spectrum difference at 30 GHz for the three waveforms.

Relatively large differences are seen above 30 GHz, but with no relevant impact on the reconstruction of the waveforms. Although the square wave presents energy at the even harmonics due to signal asymmetry, the spectrum difference at those harmonics can become large due to the low amplitude levels. As the square and sinc-like waveforms present low signal-to-noise ratio at higher frequencies, we fitted their phases only up to 30 GHz to guarantee proper phase-detrending (see Figs. 6-7).

Note the fundamental phase of the comb waveform at 180 degrees in Fig. 5b, corresponding to the inversion of the comb pulse with respect to the 10 MHz reference signal (see Fig. 5c).

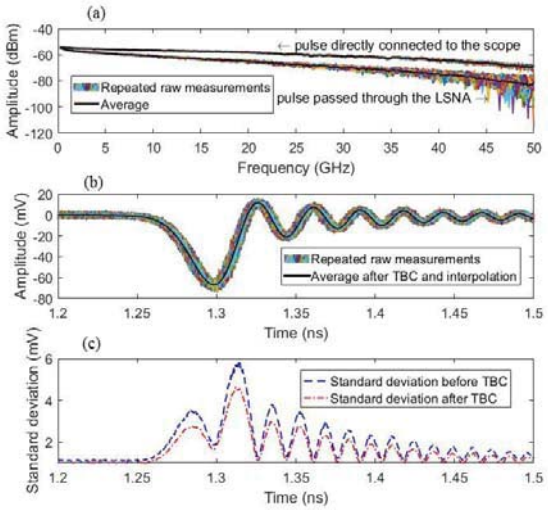

Fig. 4 a) Repeated scope measurements in the frequency domain with the comb generator directly connected to the scope and going through the LSNA test set. b) Time-domain of raw scope measurements and respective average after TBC correction. c) Standard deviation of the repeated scope measurements before and after TBC correction.

TABLE I Spectrum difference at 30 GHz and peak time-domain difference

Waveform under test	Amplitude Diff. (dB)	Phase Diff. (degrees)	Time-domain Diff. (mV)
200 MHz comb	0.3	1.6	1.5
1 GHz square	0.1	1.1	3.8
1 GHz sinc-like	1.4	7.9	4.6

V. Conclusion

We successfully compared pulse waveform measurements performed with a frequency-domain technique (LSNA) and a time-domain technique (scope). We calibrated the LSNA for operation with an external pulse source and we corrected the scope measurements to the same reference plane as the LSNA. The techniques presented will be combined with an on-wafer multiline Thru-Reflect-Line kit and a two-tier calibration approach, and applied to on-wafer cryogenic measurements.

Acknowledgement

This research was supported by NIST's Innovations in Measurement Science program. Thanks to Rich Chamberlin, Jérôme Cheron, Konstanty Lukasik, Nathan Flowers-Jacobs, Jim Booth, Kate Remley and the NIST Superconductive Electronics Group. Gustavo Avolio is a post-doctoral researcher supported by FWO Flanders (Belgium).

References

[1] Samuel P. Benz *et al*., "Low-distortion Waveform Synthesis with Josephson Junction Arrays", *Appl. Phys. Lett*., vol. 77, no. 7, 14 August 2000.

[2] N. E. Flowers-Jacobs, A. E. Fox, P. D. Dresselhaus, R. E. Schwall and S. P. Benz, "Two-Volt Josephson Arbitrary Waveform Synthesizer Using Wilkinson Dividers," in *IEEE Transactions on Applied Superconductivity*, vol. 26, no. 6, pp. 1-7, Sept. 2016.

[3] J. Scott *et al*., "Removal of cable and connector dispersion in time-domain waveform measurements on 40 Gb integrated circuits," *IEEE MTT-S International Microwave Symposium*, Seattle, WA, USA, 2002, pp. 1669-1672 vol.3.

[4] J. B. Scott *et al*., "Enhanced on-wafer time-domain waveform measurement through removal of interconnect dispersion and measurement instrument jitter," *IEEE Trans. Microwave Theory and Techniques*, vol. 50, no. 12, pp. 3022-3028, Dec 2002.

[5] D. Williams, P. Hale and K. A. Remley, "The Sampling Oscilloscope as a Microwave Instrument," in *IEEE Microwave Magazine*, vol. 8, no. 4, pp. 59-68, Aug. 2007.

[6] A. Aldoumani, P. J. Tasker, R. S. Saini, J. W. Bell, T. Williams and J. Lees, "Operation and calibration of VNA-based large signal RF I-V waveform measurements system without using a harmonic phase reference standard," 81st *ARFTG Microwave Measurement Conference*, Seattle, WA, 2013, pp. 1-4.

[7] P. D. Hale, C. M. Wang, D. F. Williams, K. A. Remley and J. D. Wepman, "Compensation of Random and Systematic Timing Errors in Sampling Oscilloscopes," in *IEEE Transactions on Instrumentation and Measurement*, vol. 55, no. 6, pp. 2146-2154, Dec. 2006.

[8] Valeria Teppati, Andrea Ferrero and Mohamed Sayed, "*Modern RF and Microwave Measurement Techniques*", Cambridge University Press, Cambridge UK, July 2013

[9] T.S. Clement, P. D. Hale, D. F. Williams, C. M. Wang, A. Dienstfrey, and D. A. Keenan, "Calibration of Sampling Oscilloscopes with High-Speed Photodiodes", *IEEE Trans. Microwave Theory and Techniques*, Aug. 6 A.D.

[10] D. F. Williams, T. S. Clement, P. D. Hale and A. Dienstfrey, "Terminology for high-speed sampling-oscilloscope calibration", *ARFTG Microwave Measurement Conference.*, vol. 68, pp. 9-14, 2006-Dec.

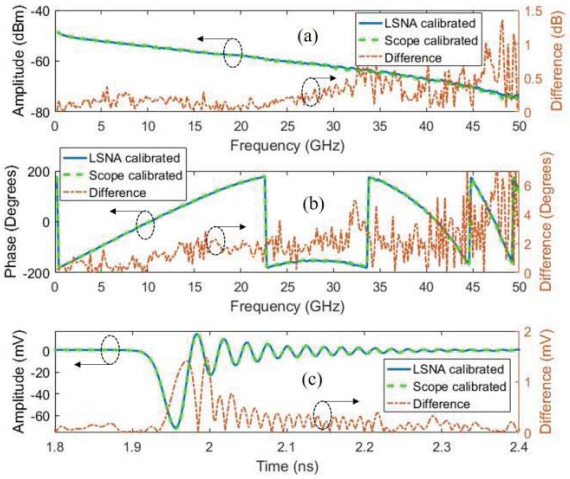

Fig. 5: 200 MHz comb pulse incident at the reference plane. a) Spectrum magnitude, b) Phase, c) Time-domain (zoom in)

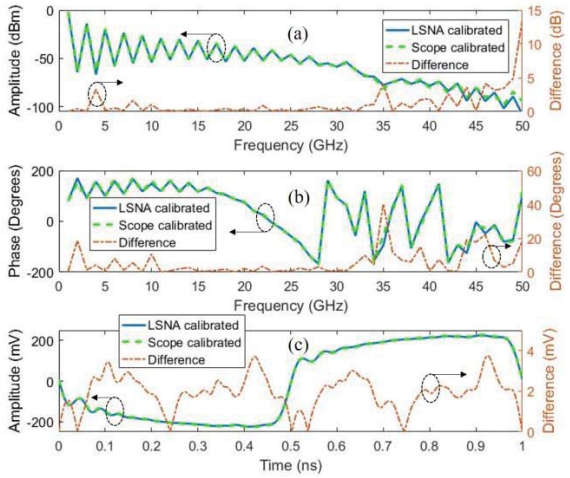

Fig. 6: 1 GHz square wave incident at the reference plane. a) Spectrum magnitude, b) Phase, c) Time-domain.

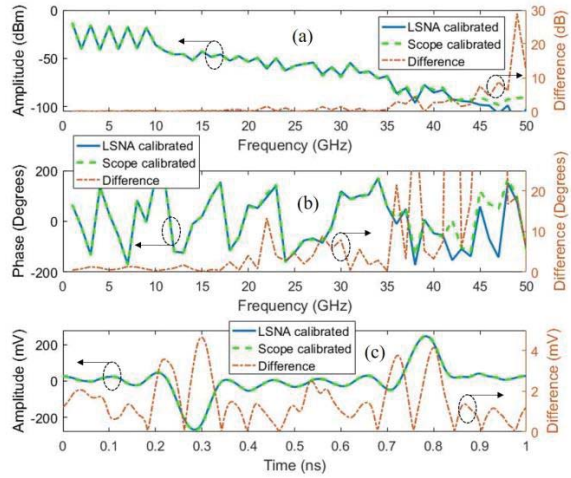

Fig. 7: 1 GHz sinc-like wave incident at the reference plane. a) Spectrum magnitude, b) Phase, c) Time-domain.